BIOLOGY OF REPRODUCTION **85,** 397–408 (2011)
Published online before print 9 March 2011.
DOI 10.1095/biolreprod.110.088591

Seminal Fluid Regulates Accumulation of FOXP3$^+$ Regulatory T Cells in the Preimplantation Mouse Uterus Through Expanding the FOXP3$^+$ Cell Pool and CCL19-Mediated Recruitment[1]

Leigh R. Guerin,[3] Lachlan M. Moldenhauer,[3] Jelmer R. Prins,[4] John J. Bromfield,[3] John D. Hayball,[5] and Sarah A. Robertson[2,3]

Research Centre for Reproductive Health,[3] School of Paediatrics and Reproductive Health, University of Adelaide, Adelaide, South Australia, Australia
Department of Obstetrics and Gynaecology,[4] University Medical Center Groningen, University of Groningen, The Netherlands
Sansom Institute,[5] School of Pharmacy and Medical Sciences, University of South Australia, Adelaide, South Australia, Australia

ABSTRACT

Regulatory T (Treg) cells facilitate maternal immune tolerance of the semiallogeneic conceptus in early pregnancy, but the origin and regulation of these cells at embryo implantation is unclear. During the preimplantation period, factors in the seminal fluid delivered at coitus cause expansion of a CD4$^+$CD25$^+$ putative Treg cell population in the para-aortic lymph nodes draining the uterus. Using flow cytometry, immunohistochemistry, and real-time quantitative PCR (qPCR) for the signature Treg cell transcription factor FOXP3, we confirmed the identity of the expanded lymph node population as FOXP3$^+$ Treg cells and showed that this is accompanied by a comparable increase in the uterus of FOXP3$^+$ Treg cells and expression of *Foxp3* mRNA by Day 3.5 postcoitum. Seminal plasma was necessary for uterine Treg cell accumulation, as mating with seminal vesicle-deficient males failed to elicit an increase in uterine Treg cells. Furthermore seminal fluid induced expression of mRNA encoding the Treg chemokine CCL19 (MIP3beta), which acts through the CCR7 receptor to regulate Treg cell recruitment and retention in peripheral tissues. Glandular and luminal epithelial cells were identified as the major cellular origins of uterine CCL19, and exposure to both seminal plasma and sperm was required for maximum expression. Together, these results indicate that Treg cells accumulate in the uterus prior to embryo implantation and that seminal fluid is a key regulator of the uterine Treg cell population, operating by both increasing the pool of available Treg cells and promoting their CCL19-mediated recruitment from the circulation into the implantation site.

cytokines, immunology, pregnancy, regulatory T cells, seminal fluid, tolerance, uterus

INTRODUCTION

A state of maternal immune tolerance is needed to avoid immune attack on the developing conceptus after implantation. This is achieved through a variety of adaptations within the immune system [1]. One such adaptation is an expansion of the suppressive CD4$^+$CD25$^+$ regulatory T (Treg) cell subset [2–4]. Treg cells mediate suppression of the proliferation and effector function of a range of leukocyte subsets including CD4 and CD8 T cells, B cells, and NK cells, as well as influence the maturation and function of dendritic cells (DCs) and macrophages [4, 5]. The importance of Treg cells in the reproductive process is highlighted in mouse models that display inability to maintain allogeneic pregnancy in their absence [2, 6].

Treg cells comprise approximately 5%–10% of CD4$^+$ T cells in rodent species and are defined by their constitutive expression of the interleukin 2 receptor-α chain (CD25) [7] and, more recently, their expression of the hallmark Treg cell marker forkhead box P3 (FOXP3) [8, 9]. The majority of Treg cells are generated within the thymus [5], and antigens within the periphery are critical in expanding thymic emigrants and inducing the de novo generation of Treg cells from naive CD4$^+$ T cells [10]. The role of fetal alloantigens in the expansion and function of Treg cells in pregnancy remains unclear [2, 3]. However, like other T cells, Treg cells require T-cell receptor (TCR) engagement and activation to fully elicit their suppressive function [11], and evidence suggests that a further consequence of TCR engagement in vivo is proliferation [12]. Therefore, it is likely that fetal antigens encountered by maternal antigen-presenting cells act to stimulate Treg cell generation, activation, and expansion.

Our recent studies suggest that delivery of male seminal fluid at coitus is involved in activating paternal antigen-reactive Treg cells at the outset of pregnancy [13]. Semen elicits an inflammation-like response and activates immune changes in many mammalian species including mice [14] and humans [15, 16]. The transmission of seminal fluid at coitus is the earliest and most frequent way in which the female immune system is exposed to paternal antigens that are later encountered on the implanting embryo. Considerable evidence supports the hypothesis that semen facilitates induction of a state of immune tolerance [17] and that this occurs in a paternal antigen-specific manner [13, 18] as a consequence of uterine DCs cross-presenting seminal fluid antigens to activate maternal T cells [19].

Previously, it has been shown that in the period between mating and embryo implantation, expansion of the CD4$^+$CD25$^+$ T cell population occurs in the para-aortic lymph nodes (LNs) that drain the uterus [13, 20] and that this expansion depends on female exposure to factors in the seminal plasma fraction of the male ejaculate [13]. However, the

[1]Supported by the National Health and Medical Research Council (NHMRC; Australia) program and fellowship grants to S.A.R.
[2]Correspondence: FAX: 61 8 83034099;
e-mail: sarah.robertson@adelaide.edu.au

Received: 15 September 2010.
First decision: 6 October 2010.
Accepted: 7 March 2011.

eISSN: 1529-7268 http://www.biolreprod.org
ISSN: 0006-3363

TABLE 1. Real-time PCR primer sequences and Genbank accession numbers.

Target mRNA[a]	Forward primer	Reverse primer	GenBank accession no.
Foxp3 (1)	5′-AGG AG AAG CTG GGA GCT ATG C-3′	3′-GTG GCT ACG ATG CAG CAA GA-5′	NM_054039
Foxp3 (2)	5′-TGC CTT CAG ACG AGA CTT GGA-3′	3′-TTC TTG GGT TAC GGG TTG G-3′	NM_054039
Ccl4	5′-CCA GGG TTC TCA GCA CCA AT-3′	3′-CAC AGC TGG CTT GGA GCA A-5′	NM_013652.2
Ccl5	5′-TGC CCA CGT CAA GGA GTA TTT-3′	3′-TCT CTG GGT TGG CAC ACA CTT-5′	NM_013653.3
Ccl19	5′-GAC CTT CCC AGC CCC AAC T-3′	3′-CGG AAG GCT TTC ACG ATG TT-5′	NM_011888.2
Ccl22	5′-CAC CCT CTG CCA TCA CGT TT-3′	3′-CCT GGG ATC GGC ACA GAT AT-5′	NM_009137.2
Ccr4	5′-CCG TAC AAC GTG GTG CTT TTC-3′	3′-TTC TGT AGC CTG GAT GGC G-5′	NM_009916.2
Ccr5	5′-GCT CCT GCC CCC ACT CTA CT-3′	3′-TCA CGC TCT TCA GCT TTT TGC-5′	NM_009917.5
Ccr7	5′-GAA ACC CAG GAA AAA CGT GCT-3′	3′-CCG TGG TAT TCT CGC CGA T-5′	NM_007719.2
Itgae	5′-TGA TCT TCA AGA GAG CCG GG-3′	3′-TCT AGG ACA TGC TGC ATG GC-5′	NM_008399.2
Actb	5′-CGT GGG CCG CCC TAG GCA CCA-3′	3′-ACA CGC AGC TCA TTG TA-5′	NM_007393.3

[a] Gene symbols and synonyms are according to nomenclature specified by Mouse Genome Informatics at http://www.informatics.jax.org/ [62].

relevance of the LN response and the significance of insemination for Treg cells in the uterus, where these cells are presumably required at implantation to exert their suppressive effector function, have not been explored. In this study, we utilized the specific Treg cell marker FOXP3 to show that there is an increase in Treg cells in the uterus prior to embryo implantation on Day 3.5 postcoitum (pc) and that uterine Treg cell accumulation depends on female exposure to seminal plasma. We also provide evidence that seminal fluid up-regulates expression of the T-cell chemokine CCL19 in uterine glandular epithelial cells in the region of Treg cell accumulation in the endometrial stroma. We conclude that the seminal plasma acts in female tissues to induce an elevation in the Treg cell population in the uterus and that this occurs due to increased availability of circulating Treg cells as well as Treg cell migration into the uterus due to expression of the chemokine CCL19 within uterine epithelial cells.

MATERIALS AND METHODS

Mice and Surgical Treatments

C57BL/6 (B6) and BALB/c mice were purchased from the University of Adelaide Central Animal Facility. Mice expressing a FOXP3-green fluorescent protein (GFP) fusion protein (*Foxp3*^{Gfp} mice) [9], kindly provided by Dr. Alexander Rudensky (Memorial Sloan-Kettering Institute, New York, NY), were back-crossed onto a B6 background for eight generations and were then maintained by breeding homozygous pairs. All mice were housed under specific pathogen-free conditions at the University of Adelaide Medical School Animal House on a 12L:12D cycle and given food and water ad libitum. All experiments were performed in accordance with the Guiding Principles for the Care and Use of Research Animals endorsed by the Society for the Study of Reproduction, with approval from the University of Adelaide Ethics Committee.

Vasectomized (VAS), seminal vesicle-deficient (SVX), and vasectomized/seminal vesicle-deficient (VAS/SVX) BALB/c male mice were prepared as previously described [21]. VAS males were proven incapable of fertilization by examination of females 8 days after mating. For experimental matings, one to three 8- to 12-week-old B6 females were caged with intact, VAS, SVX, or SVX/VAS stud males. Females that mated with intact or VAS males were checked for the presence of vaginal plugs, whereas mating with SVX males and SVX/VAS males was detected by the presence of sperm or by video recorded confirmation of coitus, respectively. The morning of confirmation of mating was termed Day 0.5 pc. Mated females were removed from males and caged in groups of up to three per cage.

Flow Cytometry

The para-aortic (iliac) LN and inguinal LN were dissected from females at estrus or on Day 3.5 pc. In some experiments, peripheral blood was drawn by cardiac puncture after administration of 2% 2.2.2-tribromomethanol anesthesia (Avertin; Sigma-Aldrich), and mesenteric and cervical LNs, spleen, and uterus were also excised. Blood was diluted 1:2 in phosphate-buffered saline (PBS) containing heparin (Sigma-Aldrich), and peripheral blood mononuclear cells were collected after centrifugation over Lympholyte (Cedarlane, Hornby, Canada) according to the manufacturer's instructions. For LNs and spleen, single-cell suspensions of lymphocytes were prepared by mechanical dispersion between glass microscope slides. Lymphocytes were suspended in a total of 1 ml of 0.1% bovine serum albumin (BSA) in PBS-0.05% sodium azide, pH 7.4 (fluorescence-activated cell sorting [FACS] buffer). For total cell quantification, a 100-μl aliquot was removed for later analysis. The remaining portion was washed and resuspended at 10^7 cells/ml. Aliquots of 10^6 cells were incubated (10 min, 4°C) with 0.5 μg of anti-Fc-γIIR antibody (FcBlock; BD Pharmingen, San Diego, CA) to block nonspecific binding. Cells were subsequently incubated (30 min, 4°C) with 0.5 μg each of PE anti-CD4 (L3T4; BD Pharmingen) and phycoerythrin (PE)-Cy7 anti-CD25 (PC61; eBioscience, San Diego, CA). In some experiments, biotinylated anti-CCR7 (eBioscience) followed by 0.2 μg of PE-Cy5 streptavidin (BD Pharmingen) were also added. Following surface staining, cells were fixed and permeabilized using the Foxp3 Staining Buffer set (eBioscience) according to the manufacturer's instructions. Permeabilized cells were incubated (30 min, 4°C) with 0.25 μg of allophycocyanin anti-FOXP3 (FJK-16s; eBioscience). After being washed with 1× fix-permeabilization buffer (eBioscience), cells were resuspended in 500 μl of fix-permeabilization buffer and analyzed with a FACSCanto flow cytometer using FACSDiva software (both, BD Biosciences).

For quantification of $CD4^+$ cell numbers, 100-μl aliquots of cells were incubated (10 min, 4°C) with 10 μl of FACS buffer containing 0.5 μg of anti-Fc-γIIR antibody, followed by incubation (30 min, 4°C) with 10 μl of FACS buffer containing 0.5 μg of PE anti-CD4. Subsequently, 20 μl of CountBright absolute counting beads (Molecular Probes, Invitrogen, Carlsbad, CA) was added with 860 μl of FACS buffer. The absolute numbers of $CD4^+FOXP3^+$ cells and $CD4^+CD25^+$ cells per LN were then calculated using the FACSCanto flow cytometer and FACSDiva software.

To evaluate CCL19 expression in uterine cells, the entire uterus was dissected and trimmed of fat and mesentery, split lengthwise, and digested in 2.5 μg/ml DNase and 1 mg/ml of collagenase A (Sigma) for 1 h at 37°C with agitation, as previously described [22]. The cell suspension was filtered and incubated (10 min, 4°C) with FcBlock followed by incubation (30 min, 4°C) with 0.5 μg each of fluorescein isothiocyanate-conjugated lectin from *Dolichos biflorus* agglutinin (DBA; Sigma), PE anti-EMR1 (F4/80; eBioscience), allophycocyanin anti-CD45, and PE-Cy7 anti-integrin, alpha M (ITGAM, CD11b; both, BD Pharmingen). Cells were fixed and permeabilized and labeled with biotinylated anti-CCL19 (30 min, 4°C) followed by PE-Cy5 streptavidin (BD Pharmingen). CCL19 expression was analyzed using the FACSCanto flow cytometer and FACSDiva software.

Quantitative Real-Time PCR

Uterine tissue was excised from estrous or Day 3.5 pc mice mated to intact, SVX, VAS, or SVX/VAS stud males, and RNA was extracted and reverse transcribed as previously described [23] and then resuspended in 100 μl of RNase-free water and stored at −20°C until required. Quantitative real-time PCR (qPCR) reactions were performed in duplicate in a final volume of 20 μl containing 10 μl of SYBR Green Master Mix (Applied BioSystems), 5 μl of H_2O, 1 μl each of 10 μM forward and reverse primers (Table 1 lists primer sequences and GenBank accession numbers), and 3 μl of cDNA template or water (as non-template negative control). Real-time qPCR conditions were 10 min at 95°C, followed by 40 cycles of 95°C for 15 sec, and 60°C for 45 sec, using an ABI Prism 7000 sequence detection system (Applied BioSystems). After DNA amplification, PCR products were subjected to melt analysis to confirm amplicon purity. Reaction products were further analyzed by electrophoresis in 2% (wt/vol) agarose gel (Promega, Madison, WI) containing 0.2 μg/ml ethidium bromide, followed by visualization over an ultraviolet light box and image capture using a Kodak digital camera to confirm expected

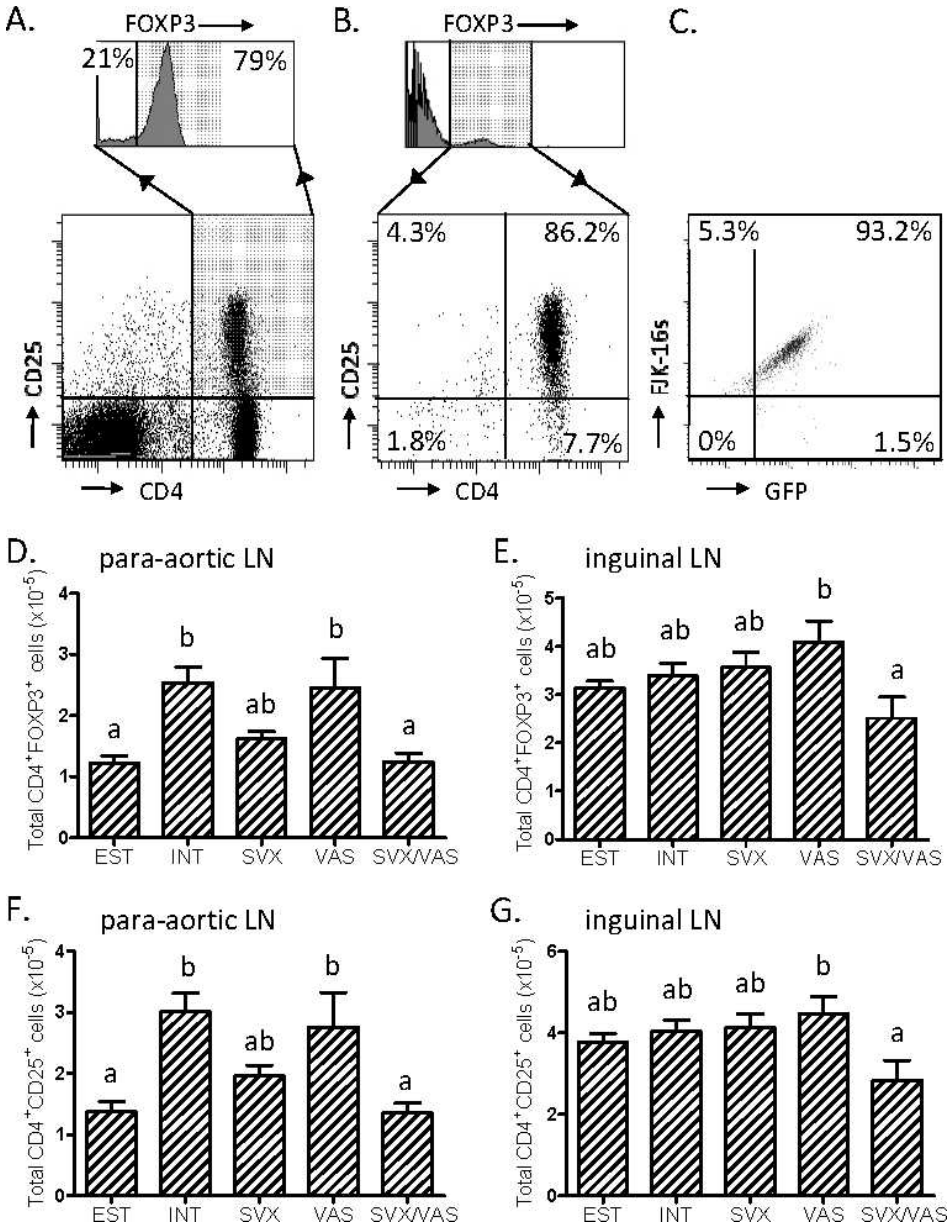

FIG. 1. The effect of seminal fluid exposure on $CD4^+FOXP^+$ and $CD4^+CD25^+$ cells in the para-aortic and inguinal LNs at Day 3.5 pc is shown. LNs were recovered from B6 virgin estrous mice (EST) or B6 mice on Day 3.5 pc after mating with intact, SVX, VAS, or SVX/VAS BALB/c males. **A**) The proportion of $CD4^+CD25^+$ cells in para-aortic LN expressing FOXP3, as detected by reactivity with FKJ-16s antibody, is shown. **B**) Expression of CD4 and CD25 in para-aortic LN $FOXP3^+$ cells, as detected by reactivity with FKJ-16s antibody, is shown. **C**) Expression of FOXP3, as detected by reactivity with FKJ-16s of GFP positivity in para-aortic LN cells from *Foxp3*^{Gfp} mice gated for expression of either FOXP3 marker is shown. Data in **A**–**C** are representative of $n \geq 4$ mice on Day 3.5 pc, and similar staining patterns were evident in $n \geq 4$ estrous mice. **D**) Absolute numbers of $CD4^+FOXP3^+$ cells in the para-aortic LNs are shown. **E**) Absolute numbers of $CD4^+FOXP3^+$ in the inguinal LNs are shown. $FOXP3^+$ cells in **D** and **E** were detected by reactivity with FKJ-16s antibody. **F**) Absolute numbers of $CD4^+CD25^+$ cells are shown in the para-aortic LNs. **G**) Absolute numbers of $CD4^+CD25^+$ in the inguinal LNs are shown. Data are means ± SEM, and different letters denote statistical significance among groups. Groups in **D**–**G** comprise n = 10–15 mice per group.

amplicon size. Assay optimization and validation experiments were performed using cDNA from murine placental tissue to define the amplification efficiency of each primer pair. Cycle threshold (Ct) values were determined for serial dilutions of cDNA, and the linearity of detection was confirmed to have a correlation coefficient of >0.99 over the detection range when plotted as Ct versus log of RNA concentration. Primer sets for target genes were acceptable if their amplification efficiency varied from that of the *Actb* housekeeper primers by <10%. All RNA samples were reverse transcribed in a single batch and were assayed with each individual primer set in the same PCR run. The *Actb* mRNA expression was shown not to vary among treatment groups. Messenger RNA abundance data were normalized to *Actb* mRNA expression using delta Ct ($\Delta Ct = Ct_x - Ct_{Actb}$) values and expressed in arbitrary mRNA units as a percentage of the mean value of the estrous control group and calibrated so that the mean of the control group was equal to 1. PCR data were then log transformed to ensure normal distribution before statistical analysis.

Immunohistochemistry

To detect FOXP3 in paraffin-embedded uterine tissue, 7-μm-thick longitudinal mid-sagittal sections were dewaxed in xylene and rehydrated. Sections were subjected to antigen retrieval by incubation in citrate buffer (10 mM sodium citrate, pH 6.0) in an autoclave (121°C, 15 psi) for 10 min. Nonspecific antibody binding was blocked by incubation (1 h, room temperature) with 10% normal rabbit serum (Sigma-Aldrich) in 1× PBS-0.025% Tween-20 (Sigma-Aldrich), and endogenous peroxidase activity was blocked by incubation for 10 min in 3% hydrogen peroxide (Sigma-Aldrich). Sections were then incubated with anti-FOXP3 (FJK-16s) primary antibody (1:400 dilution) overnight at 4°C, followed by incubation with biotinylated (1:400 dilution) rabbit anti-rat (Dako, Glostrup, Denmark) secondary antibody (1 h, room temperature). Sections were treated with streptavidin-conjugated horseradish peroxidase (Vectastain ABC kit; Vector Laboratories, Burlingame, CA) according to the manufacturer's instructions, and detection was performed using a diaminobenzidine peroxidase substrate kit (Vector Laboratories). Images were captured using a NanoZoomer 1.0 unit (Hamamatsu, Shizuoka, Japan) at a zoom equivalent of a 20× objective lens. $FOXP3^+$ cell density was quantified as the number of FOXP3-positive cells per mm^2 area of tissue (both endometrial and myometrial compartments in a total of 12 sections per mouse), which was calculated by tracing the section outline using NDP-view software (Hamamatsu) and manual counting of individual $FOXP3^+$ cells.

To colocalize CCL19 and FOXP3, the uterus was excised on Day 3.5 pc from *Foxp3*^{Gfp} mice mated with intact BALB/c males and stored in an 18% sucrose solution overnight at 4°C before being embedded in OCT compound (Tissue Tex, Naperville, IL) and frozen by immersion in liquid nitrogen-cooled isopentane. Longitudinal mid-sagittal sections (7 μm thick) were air dried, fixed in 4% paraformaldehyde, and labeled sequentially with biotinylated goat anti-CCL19 (5 μg/ml; R&D Systems), and streptavidin-Alexa Fluor 594 (1:100; Invitrogen) in a 1% solution of BSA/PBS. Sections were examined using a

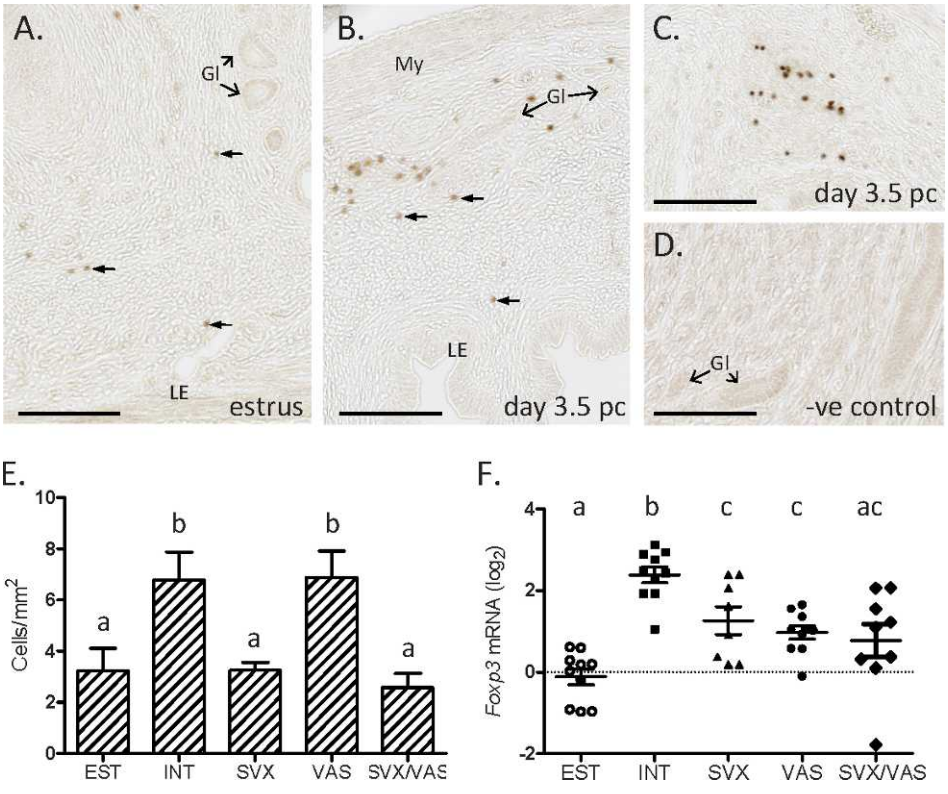

FIG. 2. The effect of seminal fluid exposure on FOXP3$^+$ cell density and *Foxp3* mRNA expression in the uterus. Uterine tissue was recovered from B6 virgin estrous mice (EST) or B6 mice on Day 3.5 pc after mating with intact, SVX, VAS, or SVX/VAS BALB/c males. Representative photomicrographs of FOXP3$^+$ cells detected by IHC with FJK-16s antibody in uterine tissue at estrus (**A**) or on Day 3.5 pc after mating with intact males (**B**, **C**), and a negative control tissue with primary antibody omitted (**D**) are shown. **A**–**D**, bar = 100 μm. LE, luminal epithelium; GI, endometrial glands; My, myometrium. Small arrows are FOXP3$^+$ cells. **E**) The effect of seminal fluid exposure on density (cells/mm^2) of FOXP3$^+$ cells in the uterine tissue, quantified by manual counting after IHC with FJK-16s antibody, is shown. Data are means ± SEM from 12 tissue sections from each of n = 5–9 mice per group. **F**) The effect of seminal fluid exposure on *Foxp3* mRNA expression in uterine tissue is shown, quantified by real-time PCR using two different primer sets for *Foxp3* (Table 1). Symbols represent the average value for the two primer sets from individual mice, and horizontal lines indicate the means ± SEM from n = 8–10 mice per group. Real-time PCR data were log transformed to a base of 2. Different letters indicate statistical significance between groups ($P < 0.05$).

Nikon C1-Z confocal microscope and EZ-C1 version 3.2 software (Tokyo, Japan).

Statistics and Data Analysis

Normally distributed data were analyzed using one-way ANOVA and Tukey post hoc test using GraphPad Prism 5 software for Microsoft Windows (GraphPad software Inc., San Diego, CA; Microsoft, Seattle, WA). When data sets were shown by the Kolmogorov-Smirnov test to be not normally distributed, nonparametric Kruskal-Wallis and Mann-Whitney *U*-tests were performed using SPSS version 13.0 software for Windows (SPSS, Inc., Chicago, IL). Individual datum points were excluded as outliers if they were greater than 2 standard deviations from the mean. Relationships between mRNA transcript abundance were analyzed by bivariate correlation using Pearson correlation coefficient R. Data are displayed as means ± standard errors of the means (SEM). Differences in groups were considered significant if *P* values were <0.05.

RESULTS

Effect of Seminal Fluid on CD4$^+$FOXP3$^+$ Cell Number in the Uterine-Draining Lymph Nodes

Recently we reported that hyperplasia in the para-aortic LN draining the uterus after mating combined with an elevation in the proportion of CD4$^+$ cells expressing CD25 resulted in a greater than 2-fold increase in the number of CD4$^+$CD25$^+$ cells [13]. We reported that 90% of the CD4$^+$CD25$^+$ cells in para-aortic LN express FOXP3 [13], and other studies have shown that these CD4$^+$CD25$^+$ cells exert immune-suppressive activity in vitro [2, 3], implying they are Treg cells; however, the CD4$^+$CD25$^+$ subset may also contain newly activated T cells other than Treg cells, so the extent to which Treg cells comprise the expanded cell population has not been formally defined.

In this study, an anti-FOXP3 antibody and single tube cell quantification method were used to more precisely define para-aortic LN Treg cells as CD4$^+$FOXP3$^+$ cells. Initially, flow cytometry analysis was performed with cells stained for surface CD4 and CD25 and then fixed, permeabilized, and stained with anti-mouse FOXP3 antibody FJK-16s. Of the total CD4$^+$CD25$^+$ cell subset, approximately 80% of cells were colabeled with FJK-16s (Fig. 1A). Of the total FJK-16s reactive population, 86% of cells expressed both CD4 and CD25, 8% of cells were CD4$^+$CD25$^-$, 4% of cells were CD4$^-$CD25$^+$, and 2% of cells were CD4$^-$CD25$^-$ (Fig. 1B). This staining distribution was similar in all estrous and mated mice evaluated (n ≥ 4 per group). To confirm that the antibody FJK-16s specifically labeled FOXP3$^+$ cells, para-aortic LN cells from *Foxp3^{Gfp}* mice were fixed and permeabilized and then labeled with FJK-16s. Of the cells that expressed the FOXP3-GFP fusion protein, 99% of cells were labeled by FJK-16s, whereas conversely, 95% of cells labeled by FJK-16s expressed the FOXP3-GFP fusion protein. Of the cells positive for either FOXP3-GFP expression or labeled by FJK-16s, 93.2% of cells were positive for both markers (Fig. 1C). These data demonstrate that positivity for FJK-16s staining is a reasonable marker of FOXP3 expression in para-aortic LN cells and show that despite substantial overlap between CD4$^+$CD25$^+$ cells and CD4$^+$FOXP3$^+$ cells, there is not complete identity between these two populations.

We then assessed the consequence of seminal fluid exposure at mating for the CD4$^+$FOXP3$^+$ and CD4$^+$CD25$^+$ cell populations in the para-aortic LN on Day 3.5 pc and, for comparison, included cells from the inguinal LN, which does not drain the uterus. Compared to virgin estrous animals, there was a 2.2-fold increase in the absolute number of CD4$^+$FOXP3$^+$ cells in the para-aortic LNs of B6 females mated to intact BALB/c males ($P < 0.01$) (Fig. 1D). This was not seen in the inguinal LNs, where no significant differences in CD4$^+$FOXP3$^+$ cell numbers were observed at Day 3.5 pc between intact-mated mice and virgin mice (Fig. 1E).

To assess the relative contributions of sperm and seminal plasma fractions of the ejaculate in expanding the CD4$^+$FOXP3$^+$ cell population, we mated females with VAS,

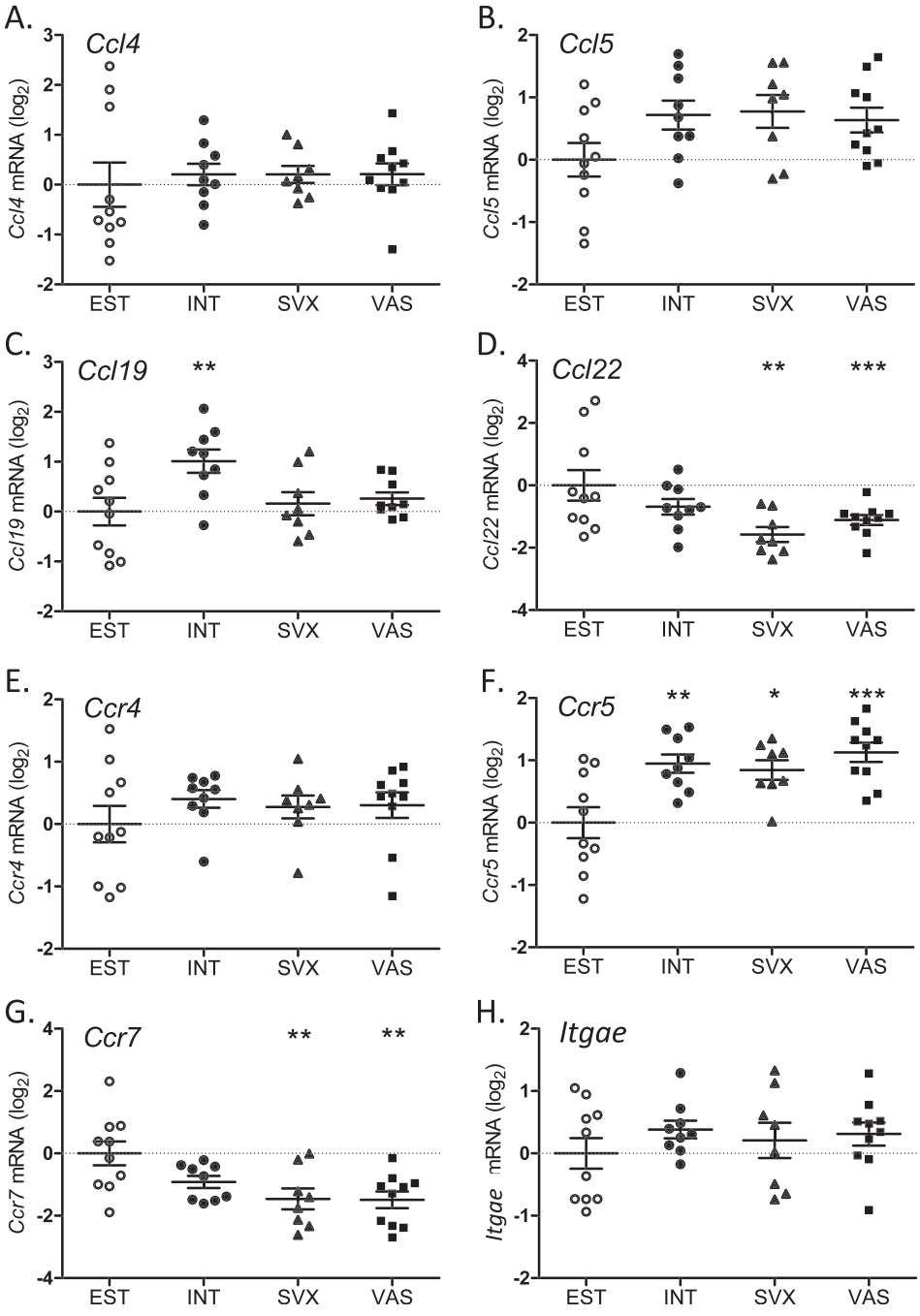

FIG. 3. The effect of seminal fluid exposure on expression of mRNAs encoding chemokines and chemokine receptors in uterine tissue at Day 3.5 pc is shown. Uterine tissue was recovered from B6 virgin estrous mice (EST) or B6 mice on Day 3.5 pc after mating with intact, SVX, or VAS BALB/c males. Expression of (**A**) *Ccl4*, (**B**) *Ccl5*, (**C**) *Ccl19*, (**D**) *Ccl22*, (**E**) *Ccr4*, (**F**) *Ccr5*, (**G**) *Ccr7*, and (**H**) *Itgae* mRNAs in uterine tissue were measured by real-time qPCR using primer sets detailed in Table 1. Symbols represent values for individual mice, and horizontal lines indicate the means ± SEM from n = 8–10 mice per group. Real-time PCR data were log transformed to a base of 2. The effect on the treatment group was analyzed by one-way ANOVA and Tukey post hoc tests; *, $P < 0.05$; **, $P < 0.01$; ***, $P < 0.001$, compared with the estrous (EST) group.

SVX, or SVX/VAS BALB/c males. In the para-aortic LNs, expansion of the $CD4^+FOXP3^+$ cell population was dependent on the seminal plasma but not on the sperm fraction of the ejaculate, as mating with seminal plasma-deficient (SVX or SVX/VAS) males resulted in no increase in the number of $CD4^+FOXP3^+$ cells compared to those in virgin estrous animals (Fig. 1D). Conversely, mating with VAS studs resulted in an increase in $CD4^+FOXP3^+$ cells ($P < 0.01$) that was similar to that in intact-mated mice. In the distal inguinal LNs, there were no significant differences between any of the mated groups compared to virgin estrous mice (Fig. 1E). This implicates local events in the uterine tissue, rather than systemic endocrine events associated with mating, in driving expansion of the para-aortic LN $CD4^+FOXP3^+$ cell population.

Among $CD4^+CD25^+$ cells, the magnitude of change for each mating group relative to that of the estrous mice was similar or slightly greater than that seen in $CD4^+FOXP3^+$ cells (Fig. 1, D and E). This is consistent with the considerable but not complete overlap between the two populations and is likely accounted for by the presence of activated T cells other than $FOXP3^+$ cells in the $CD4^+CD25^+$ pool.

Effect of Seminal Fluid on FOXP3$^+$ Cell Number and Foxp3 *mRNA Expression in the Peri-Implantation Uterus*

Next, we investigated whether the increase in Treg cells in the para-aortic LNs was accompanied by an elevation in FOXP3 cells in the uterus on Day 3.5 pc. To address this, the density of $FOXP3^+$ cells in Day 3.5 pc uterine tissue recovered from B6 mice mated to either intact, SVX, VAS, or SVX/VAS

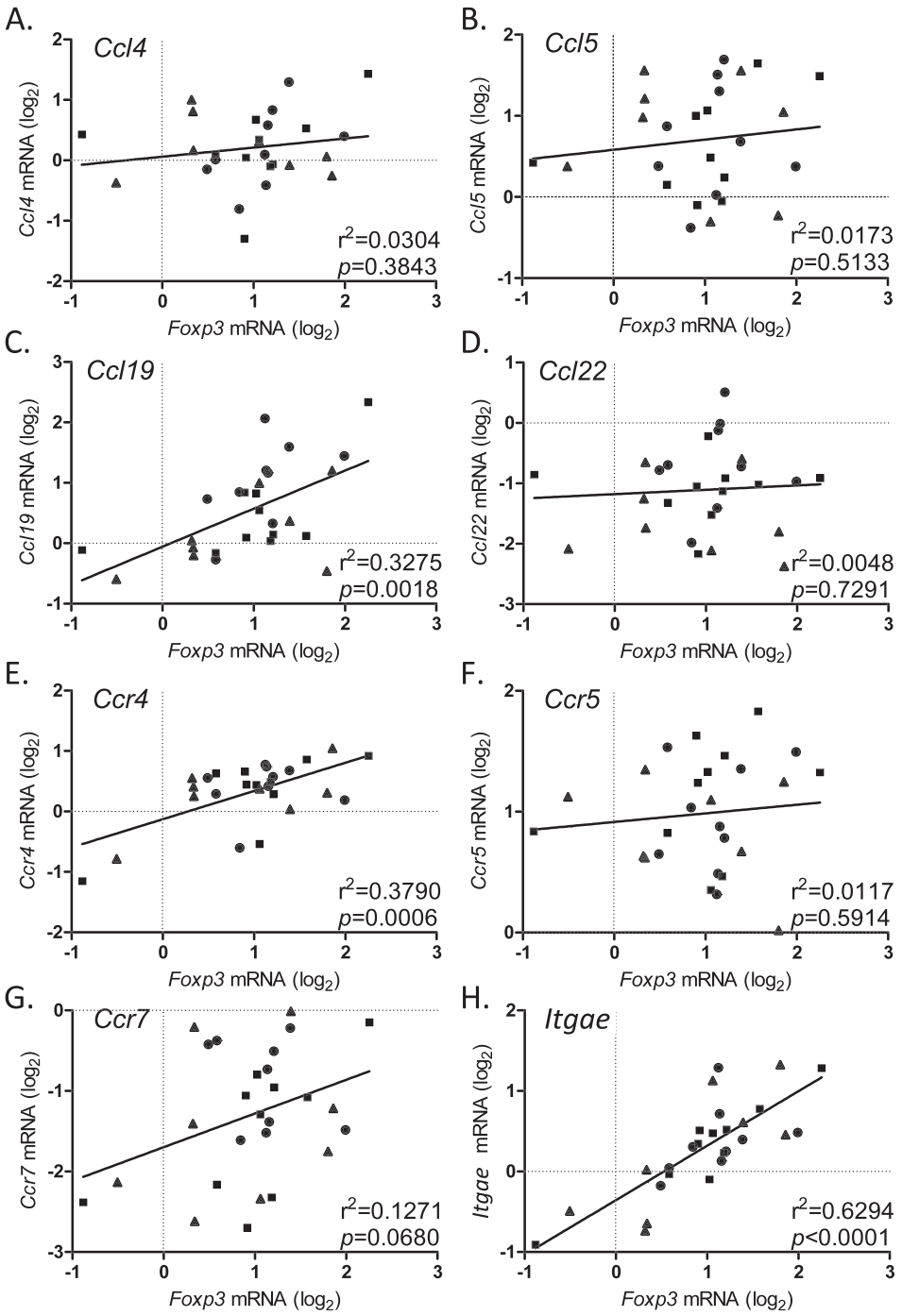

FIG. 4. Correlations between mRNAs encoding chemokines and chemokine receptors and *Foxp3* mRNA in Day 3.5 pc uterine tissue are shown. Uterine tissue was recovered from B6 mice on Day 3.5 pc after mating with intact, SVX, or VAS BALB/c males, and mRNAs were measured by real-time qPCR as shown in Figures 2 and 3. Linear regression analysis was performed to assess the correlation between abundance of *Foxp3* mRNA and abundance of (**A**) *Ccl4*, (**B**) *Ccl5*, (**C**) *Ccl19*, (**D**) *Ccl22*, (**E**) *Ccr4*, (**F**) *Ccr5*, (**G**) *Ccr7*, and (**H**) *Itgae* mRNAs in uterine tissue. Symbols represent the expression of *Foxp3* mRNA (x axis) against the chemokine or chemokine receptor transcript of interest (y axis) for the same tissue sample. Circles, triangles, and squares represent data from the INT, SVX, and VAS groups, respectively. The relationship between transcript abundance was analyzed by bivariate correlation using Pearson correlation coefficient R. The coefficient of determination is indicated as the r^2 value, and *P* values are shown.

BALB/c males was analyzed using immunohistochemistry (IHC) and compared to that in virgin estrous mice. In tissue from estrous mice, $FOXP3^+$ cells were sparsely distributed individually or in clusters throughout the endometrial tissue, with fewer cells in the myometrial tissue (Fig. 2A). Tissue from Day 3.5 pc mice mated with intact males contained more $FOXP3^+$ cells, which were frequently clustered in the endometrial stroma, predominantly in the deeper regions and rarely located in the superficial stroma subjacent to the luminal epithelium or in the myometrium (Fig. 2, B and C).

Quantification showed that in uterine tissue from mice mated with intact males, the density of cells expressing FOXP3 was 2.1-fold increased ($P < 0.05$) compared with that in estrous mice (Fig. 2E). Tissue from females mated with VAS males displayed a similar pattern of location (not shown) and comparable increase in density of $FOXP3^+$ cells (2.1-fold; $P < 0.05$), whereas SVX- and SVX/VAS-mated mice showed no change in $FOXP3^+$ cell number compared with estrous mice (Fig. 2E).

Real-time qPCR analysis showed a significant increase in the relative amount of *Foxp3* mRNA in the uterine tissue of mice mated with intact males compared to that in virgin estrous mice (5.6-fold; $P < 0.001$). Smaller increases were seen in uterine tissue from females mated with VAS and SVX males (2.1-fold and 2.9-fold, respectively; both, $P < 0.01$), whereas there was no significant increase seen when females were mated with SVX/VAS males. Similar results were obtained for each of the two different primer sets for *Foxp3* (data not

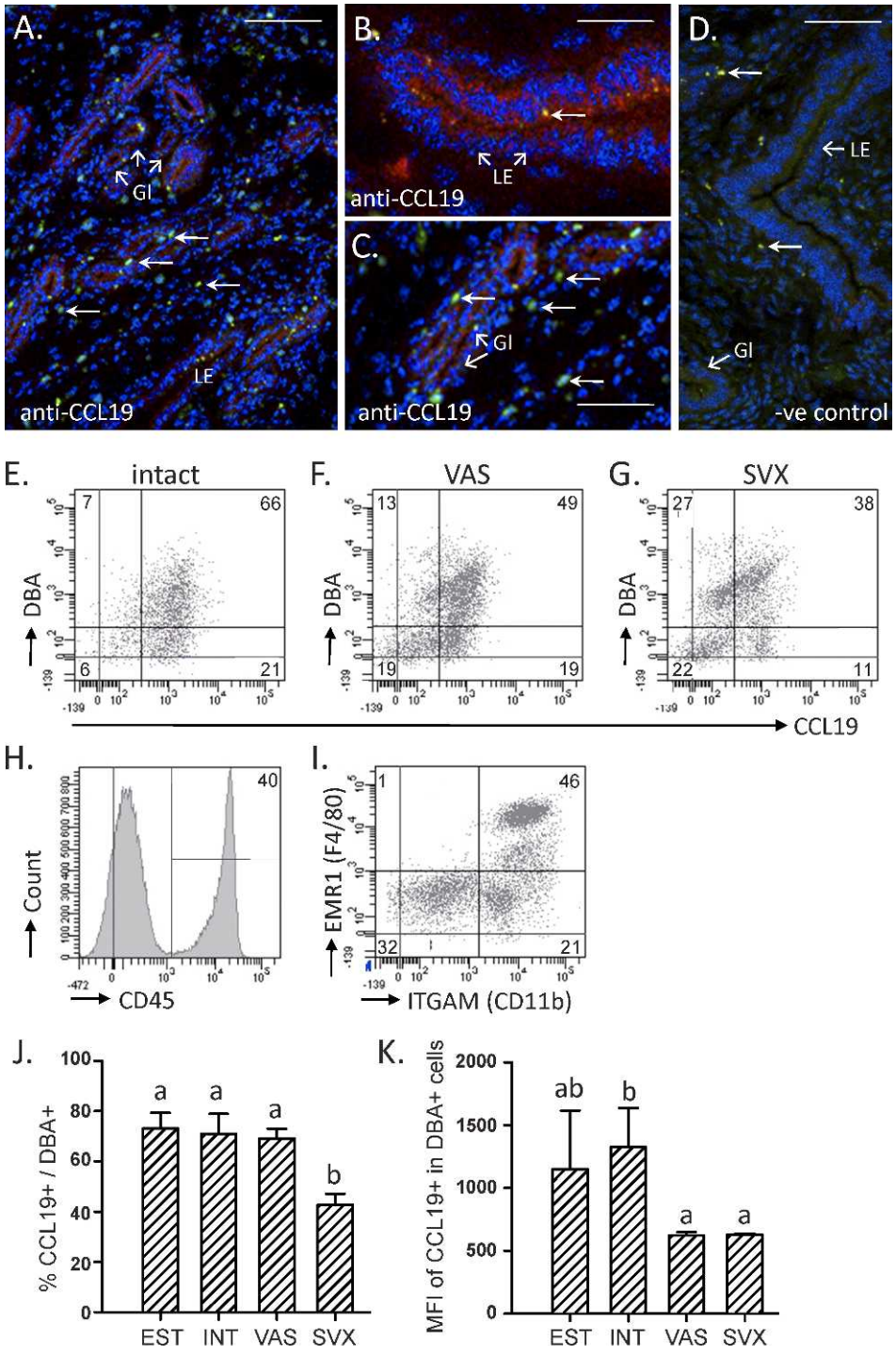

FIG. 5. Immunolocalization and flow cytometric analysis of CCL19 expression in the uterus on Day 3.5 pc are shown. CCL19 protein was localized by IHC using anti-CCL19 antibody in sections of uterine tissue recovered on Day 3.5 pc from *Foxp3*^{GFP} mice mated with intact males, enabling colocalization of CCL19 and FOXP3$^+$ cells. Representative photomicrographs of CCL19 in uterine tissue (**A**, **B**, **C**) and a negative control tissue with irrelevant primary antibody (**D**) are shown. Bar = 50 μm for **A** and **D**; bar = 100 μm for **B** and **C**. LE, luminal epithelium; GI, endometrial glands. Large arrows are FOXP3$^+$ cells (green staining) and CCL19 immunoreactivity is evident in luminal epithelium and glandular epithelium (red staining). CCL19$^+$ cells were analyzed for coexpression of the epithelial cell-reactive lectin DBA or leukocyte markers CD45, EMR1 (F4/80), and ITGAM (CD11B) in uterine cell suspensions recovered from B6 females on Day 3.5 pc after mating to intact, VAS, or SVX males (**E**–**K**). Representative FACS plots show that the majority of CCL19$^+$ cells recovered from females mated with intact (**E**), VAS (**F**), or SVX males (**G**) also reacted with DBA, with the number in each corner indicating the percentage of cells within that quadrant. The DBA$^-$CCL19$^+$ population was analyzed for CD45$^+$ expression (**H**), and the CCL19$^+$CD45$^+$population was analyzed for the macrophage markers ITGAM and EMR1 (**I**). The percentage of DBA$^+$ epithelial cells expressing CCL19 (**J**) and their intensity of CCL19 expression (**K**) were quantified by flow cytometry. Data are the means ± SEM from n = 4–6 mice per group. Data were analyzed by Kruskal-Wallis and Mann-Whitney *U*-tests, and different letters indicate statistical significance between groups ($P < 0.05$).

shown), so data reported herein are from mean values for the two primer sets.

Effect of Seminal Plasma on Uterine Expression of mRNAs Encoding Chemokines and Chemokine Receptors

To investigate the possible role of chemokines in uterine accumulation of FOXP3$^+$ cells in the preimplantation period, we then assessed expression of mRNAs encoding a range of chemokines and chemokine receptors in uterine tissue collected at estrous and at Day 3.5 pc after mating with intact, VAS, SVX, or VAS/SVX males. Chemokines shown previously to be involved in Treg cell migration in tissue sites other than the uterus were chosen for analysis. These included the *Ccl4*, *Ccl5*, *Ccl19*, and *Ccl22* chemokine ligands and the *Ccr4*, *Ccr5*, and *Ccr7* chemokine receptors. In addition, we measured the *Itgae* mRNA encoding the key Treg cell-retaining integrin CD103 [24]. Of these, the *Ccl19* and *Ccr5* chemokines were shown to increase expression following mating to intact males (2.0-fold, $P < 0.01$; and 1.8-fold, $P < 0.01$, respectively) (Fig. 3, C and F). A strong trend toward increased *Ccl5* expression (encoding CCL5, RANTES) was also seen (1.5-fold, $P = 0.06$) (Fig. 3B).

The increase in *Ccl19* expression was dependent on exposure to both seminal plasma and sperm, as expression was not increased when females were mated with VAS or SVX males (Fig. 3C). Conversely, increased *Ccr5* expression was

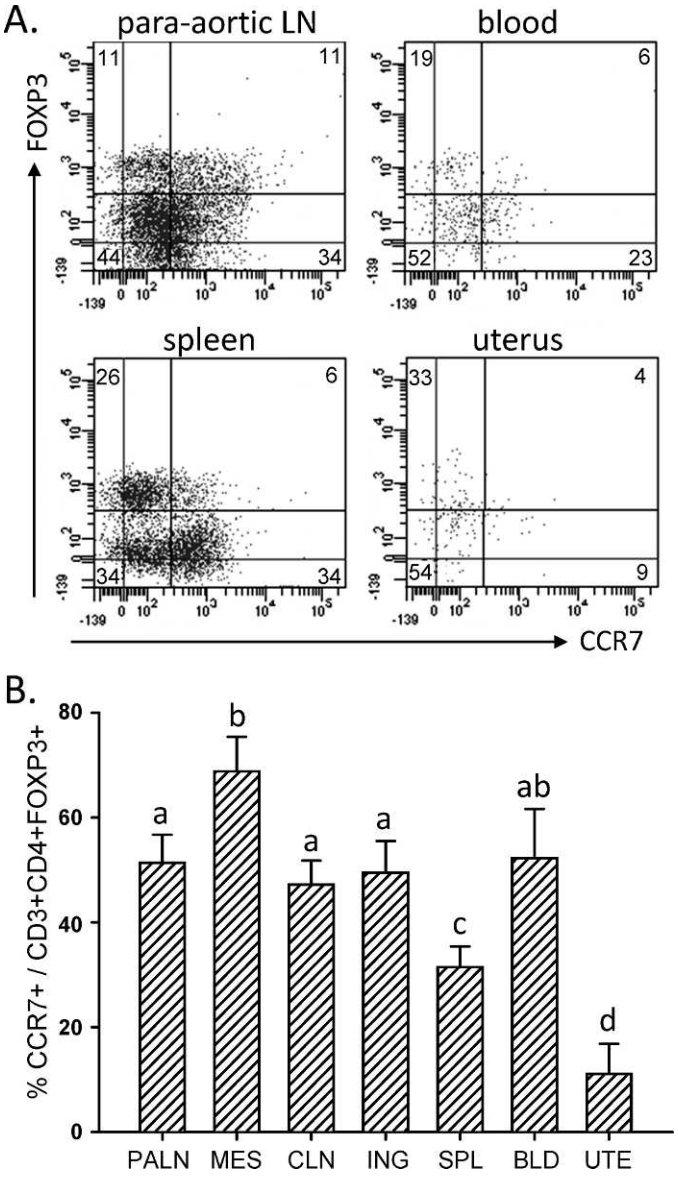

FIG. 6. Expression of CCR7 in Treg cells in early pregnancy is shown. B6 females were mated to intact BALB/c males, and the percentage of $CD3^+CD4^+FOXP3^+$ Treg cells expressing CCR7 was determined by flow cytometry in the para-aortic LN (PALN), mesenteric LN (MES), cervical LN (CLN), inguinal LN (ING), spleen (SPL), blood (BLD), and uterus (UTE). **A**) Representative plots of staining in para-aortic LN, blood, spleen, and uterus are shown, with the number in each corner indicating the percentage of cells within that quadrant. **B**) Data are the mean percentages ± SEM of $CCR7^+$ cells from n = 5–7 mice per group. Data were analyzed by Kruskal-Wallis and Mann-Whitney *U*-tests, and different letters indicate statistical significance between groups ($P < 0.05$).

independent of seminal fluid exposure, and elevated expression was also seen in tissue from mice mated with SVX males (1.8-fold, $P < 0.05$) and VAS males (2.2-fold, $P < 0.001$) (Fig. 3F). Similarly there was no effect of sperm or seminal plasma deficiency on *Ccl5* expression (Fig. 3B). In contrast, expression of both *Ccl22* and *Ccr7* mRNAs at Day 3.5 pc declined to below levels at estrus, unless females were exposed to both seminal plasma and sperm (Fig. 3, D and G).

To further examine whether changes in the expression of mRNAs encoding migratory regulators might be causally related to *Foxp3* mRNA levels in uterine tissue from mated mice, we also analyzed correlations between *Foxp3* mRNA and the chemokine and chemokine receptor mRNAs in uterine tissue from all groups of mated mice. This analysis revealed that the *Ccl19* chemokine was significantly correlated with *Foxp3* expression ($P = 0.002$; $r^2 = 0.32$) (Fig. 4C), while *Ccr5* expression was not ($P = 0.59$; $r^2 = 0.01$) (Fig. 4F). Additionally, levels of *Ccr4* and particularly *Itgae* expression were both significantly correlated with *Foxp3* expression ($P < 0.001$, $r^2 = 0.38$; and $P < 0.001$, $r^2 = 0.63$, respectively), and there was a trend toward a correlation between *Ccr7* and *Foxp3* expression ($P = 0.068$; $r^2 = 0.13$) (Fig. 4G).

Cellular Origin of Chemokine CCL19 in Uterine Tissue

Because uterine CCL19 was shown to be induced in early pregnancy and regulated by seminal fluid, we sought to investigate the cellular origin of CCL19 in uterine tissue and its spatial relationship with uterine $FOXP3^+$ cells during the preimplantation period. IHC was utilized to detect CCL19 in fresh frozen uterine tissue from $Foxp3^{Gfp}$ mice collected on Day 3.5 pc after mating with intact wild-type males, to allow colocalization of CCL19 and GFP-expressing $FOXP3^+$ cells. CCL19 staining was evident at the apical and basal surface and to a lesser extent in the cytoplasm of most glandular and luminal epithelial cells in all (n = 6) uterine tissues examined, although there was spatial variation within individual tissues in the intensity of staining. $FOXP3^+$ cells were present in the endometrial stromal tissue and were frequently located adjacent to $CCL19^+$ glandular epithelial cells and to a lesser extent adjacent to luminal epithelial cells (Fig. 5, A–C).

We further investigated the identity of cells expressing CCL19 by using flow cytometry. Using the lectin DBA as a marker of epithelial cells, we confirmed that CCL19 is expressed by >80% of epithelial cells recovered from B6 females on Day 3.5 pc after mating with intact BALB/c males (Fig. 5D). A similar percent positivity for CCL19 expression was seen in DBA^+ cells recovered from mice mated with VAS males (Fig. 5, E and I). In contrast, fewer DBA^+ epithelial cells were positive for CCL19 on Day 3.5 pc after mating with SVX males (Fig. 5, F and I). The mean fluorescent intensity of CCL19 in DBA^+ cells was higher in females mated with intact males than in females mated with VAS or SVX males (Fig. 5K). These results indicate that seminal plasma increases both the proportion of epithelial cells expressing CCL19 and the intensity of CCL19 expression.

Approximately 25% of the uterine cells expressing CCL19 were DBA negative. Flow cytometry confirmed that many of the DBA^-CCL19^+ cells were $CD45^+$ leukocytes (Fig. 5G), mainly $ITGAM^+EMR1^-$ DCs or $ITGAM^+EMR1^+$ macrophages (Fig. 5H).

Expression of the CCL19 Receptor CCR7 in Treg Cells

To determine whether Treg cells express the CCL19 receptor CCR7 in early pregnancy, B6 females were mated with intact BALB/c males, and, on Day 3.5 pc, LNs, spleen, uterus, and blood were collected for flow cytometry. Expression of CCR7 was clearly evident in $CD4^+CD25^+FOXP3^+$ Treg cells collected from para-aortic and peripheral LNs, blood, and spleen, but of the small numbers of Treg cells detectable in the uterus, few expressed the CCR7 receptor (Fig. 6A). Within the para-aortic, mesenteric, cervical, and inguinal LNs and blood, the majority of Treg cells (50%–70%) were positive for CCR7; however, significantly fewer uterine Treg cells expressed CCR7 (mean of

11% ± 6% SEM) than all other tissues examined ($P < 0.05$) (Fig. 6B).

DISCUSSION

Prevention of deleterious immune responses against fetal antigens is critical for pregnancy success. Despite reduced antigenicity of conceptus tissue, maternal T cells still recognize and respond to fetal antigens [19, 25, 26], potentially as part of a biological ''quality control'' mechanism to assure conceptus health [27]. $CD4^+CD25^+$ Treg cells have been identified as a T-cell subset that actively mediates maternal tolerance, and these cells are essential in the pre- and peri-implantation periods for establishing allogeneic pregnancy [2, 6], with insufficient Treg cells leading to implantation failure or miscarriage [6]. In this study we confirmed that exposure of the female reproductive tract to semen, specifically the seminal plasma component of the ejaculate, leads to a localized expansion of the $FOXP3^+$ Treg cell population in the uterus-draining para-aortic LNs, and we extended this finding to show an associated increase in $FOXP3^+$ Treg cells in the uterus at the time of embryo implantation. Additionally, we identified a role for seminal plasma-induced expression of the chemokine CCL19 in regulating uterine Treg cell accumulation prior to embryo implantation.

Exposure of the female reproductive tract to seminal fluid at mating can promote paternal antigen-specific hyporesponsiveness, ultimately inducing a state of transient active immune tolerance in the mother [13, 18, 28]. At least in part, this mechanism is mediated by Treg cells, which exert their actions at the time of embryo implantation [6, 13, 29]. TGFB and other factors in male seminal plasma, acting together with cycle-related fluctuations in ovarian steroid hormones, have been implicated in eliciting increases in paternal antigen-reactive Treg cells in local LNs during the peri-conceptual period [13, 30].

Previous studies that analyzed Treg cells over gestation have generally relied on identifying Treg cells based on the coexpression of CD4 and CD25 [2, 3, 13, 31, 32]. However CD25 expression on $CD4^+$ cells is not an exclusive marker for Treg cells and also identifies activated $CD4^+$ T cells [33], which could reasonably be increased in response to the antigenic stimulus of seminal fluid. Evidence of induction of other activation markers such as CD69 following insemination [14] brings into question whether elevations in the $CD25^+$ population simply reflects an increase in activated T cells and limits the certainty of conclusions based on this identification strategy. Therefore, the hallmark Treg cell marker FOXP3 [8, 9] offers a superior marker for identifying Treg cells among the $CD4^+$ T cell subset.

A population of $CD4^+FOXP3^+$ cells was identified that predominantly express CD25, with more than 80% of the $CD4^+CD25^+$ cell population also expressing FOXP3. However, a distinct population of $CD4^+CD25^+$ cells did not express FOXP3, suggesting that at least some of these cells are activated T cells other than Treg cells. As well, there was an additional population of $CD4^+FOXP3^+$ cells that did not express CD25. Critically, these $FOXP3^+CD4^+CD25^-$ cells have also been shown to have suppressive function [34], and thus, we assert that definitive Treg cells in reproductive tissues are most precisely identified as $CD4^+FOXP3^+$ cells. When cells were quantified according to the alternative classification phenotype of $CD4^+CD25^+$ cells, the two data sets were comparable. This indicates that conclusions drawn in earlier work with Treg cells in early pregnancy, where the Treg cells are defined as $CD4^+CD25^+$ cells, are probably valid.

In agreement with previous observations [13], on Day 3.5 pc, the total number of $CD4^+CD25^+$ cells in the uterus-draining para-aortic LNs was greater than 2-fold increased following mating to intact males. A similar result was shown when Treg cells were defined as $CD4^+FOXP3^+$cells. Also consistent with earlier findings [13] was the observation that expansion of the Treg cell population following mating occurred only in the para-aortic LNs, with the inguinal LNs and spleen (data not shown) showing no significant increase in total Treg cells. Expansion was largely attributable to introduction of seminal plasma at the time of mating, confirming a critical role in $FOXP3^+$ Treg cell expansion for the immunoreactive moieties within seminal plasma.

Treg cell numbers are higher during early pregnancy after allogeneic mating than after syngeneic mating [3]. Male antigen in the acellular fraction of the ejaculate [35] presented in the context of immunity-deviating factors such as TGFB [36] is likely to drive the postmating expansion in Treg cells in an antigen-specific manner. Experiments with mice expressing transgenic TCRs have shown that maternal antigen-presenting cells cross-present antigens from the ejaculate in the para-aortic LNs [19] and that seminal fluid-induced CSF2 (GM-CSF) facilitates this [22]. Observations that prevention of abortion in the CBA/J × DBA mating combination can be achieved if Treg cells are adoptively transferred from pregnant females, but not virgin females, are consistent with this hypothesis. Further support comes from the demonstration that paternal strain-specific tolerance of tumor cells is conferred by mating with intact but not SVX males, even in the absence of an ensuing pregnancy [13].

The largely contact-dependent mechanism of action of Treg cells dictates that their spatial distribution is critical to their suppressive function [37, 38]. For an optimal suppressive environment that would allow tolerance of the developing embryo, Treg cells would be required at the point of first contact between the conceptus and immune effector cells at implantation. Our observation of greater than 5-fold increase in *Foxp3* expression and 2-fold increase in $FOXP3^+$ cells in the endometrial stroma immediately prior to trophoblast cell penetration of the epithelial surface at implantation seems consistent with such a role. Seminal plasma appeared to be particularly important for achieving this increase in uterine Treg cells. This is thought to reflect the critical role for TGFB originating in the seminal vesicles for inducing Treg cells, an interpretation supported by experiments showing that exogenous TGFB delivered vaginally at mating can increase Treg cell numbers and alleviate abortion in CBA × DBA-mated mice [30]. A role for sperm cannot be discounted as *Foxp3* mRNA expression was diminished after mating with vasectomized males, although IHC data did not support this. It is not clear why there was a difference in requirement for sperm in the RNA and protein analyses, but differences in per-cell expression of *Foxp3* RNA depending on seminal fluid composition could account for this.

$CD4^+FOXP3^+$ cells generated in the para-aortic LNs would expand the circulating pool available to home into the uterus. The para-aortic LN are likely to be a primary site of Treg cell production and control, as the absolute numbers of Treg cells in this tissue are approximately 10-fold greater than in the entire uterus on Day 3.5 pc. In this and previous studies [13], the para-aortic LN contained approximately 3×10^5 Treg cells on Day 3.5 pc. Based on the observed density of 7 $FOXP3^+$ cells per mm^2 in uterine sections, we estimate the entire uterus contains approximately 4×10^4 Treg cells on Day 3.5 pc. Previous studies have shown that radiolabeled

para-aortic LN cells are recruited via the blood into the uterus in early pregnancy [14].

Like other T cells, the migration and trafficking of Treg cells into peripheral tissues is largely dependent on the local expression of chemokines and the presence of the cognate chemokine receptor on the surface of the Treg cell [39–41]. In the postmating period, there are coordinated changes in the level of several chemokines synthesized in the uterus, and this occurs in concert with the influx of a range of leukocytes including neutrophils, macrophages and DCs as well as T cells [42, 43].

In both the cycling nonpregnant uterus and the mid-gestation pregnant uterus (gestational Day 10.5), changes in chemokine mRNAs have been shown to occur in parallel with increased *Foxp3* mRNA [44]. To investigate which chemokines were involved in Treg cell recruitment in the peri-implantation period, we assessed uterine expression of mRNAs encoding a range of chemokine ligands and receptors and the integrin CD103, which are implicated in recruiting Treg cells [24, 41, 44–46]. Of the migratory molecules analyzed, CCL19 (also known as the macrophage inhibitory protein 3β [MIP3β]) displayed a pattern of regulation most consistent with a role in Treg cell migration. Uterine *Ccl19* mRNA was elevated during the preimplantation period and was responsive to both the sperm and seminal plasma components of the ejaculate. A functional contribution to uterine Treg cell recruitment is suggested by the positive correlation between *Ccl19* and *Foxp3* mRNA levels. Flow cytometry and immunohistochemistry confirmed the presence of CCL19, produced mainly by uterine and glandular epithelial cells, while macrophages and DCs also contributed to CCL19 production in the early pregnant uterus.

CCL19-facilitated T-cell migration is known to occur primarily as a result of its interaction with the receptor CCR7 [46]. The trend in correlation between *Ccr7* and *Foxp3* mRNA expression in the Day 3.5 pc uterus suggests this chemokine receptor is linked to Treg cell recruitment. CCL19 has been shown to induce migration of $CD62L^+$ cells, with $CD62L^+$ Treg cells displaying both preferential migration toward CCL19 and enhanced suppressive capabilities [47]. The *Cd62l* mRNA was not assessed in this study, but this potentially important subset of Treg cells warrants further investigation.

Under noninflammatory conditions, CCL19 is expressed almost exclusively in secondary lymphoid organs [48, 49]. CCL19 expression is also documented in peripheral tissues including the intestinal tract [50] and pancreas [51] and is critical for T-cell recruitment across the blood–brain barrier and into the central nervous system [52, 53]. Interestingly CCL19 is reported in the human uterus, where it is produced by luminal and glandular epithelial cells, as well as leukocytes in the endometrial stroma, with elevated expression in the late secretory phase, suggesting a role in controlling lymphocyte populations associated with implantation [54]. To date, a *Ccl19* null mutant mouse has not been reported, but ectopic transgenic synthesis of CCL19 in the pancreas causes formation of lymphoid aggregates [55], raising the possibility of CCL19 involvement in formation of the organized lymphoid structures present in the endometrium [56].

The small percentage of Treg cells expressing CCR7 in the uterus is consistent with observations that activated T cells that migrate into other peripheral tissues show a reduced CCR7 expression [57]. This downregulation in CCR7 expression may be critical in ensuring that Treg cells are retained within the uterus once recruited. This notion fits with reports that null mutation in CCR7 expression disrupts T cell emigration and causes their aberrant accumulation in the skin [58]. Disruption of CCR7-mediated transit of Treg cells through peripheral tissues is associated with a range of autoimmune disorders, but the extent to which signaling by CCL19 and the alternate CCR7 ligand CCL21 contribute is not resolved [46].

Previous studies have implicated CCR5 expression by Treg cells and uterine expression of the CCR5 ligand CCL4 as promoting selective migration into the gravid uterus, although no deficiency in uterine Treg cells in *Ccr5* null mutant mice implies redundancy with other Treg cell chemokine receptors [44, 59]. We showed no change in uterine *Ccl4* expression in early pregnancy; however, elevated *Ccr5* expression was evident, irrespective of seminal plasma exposure and so potentially attributable to the effects of ovarian steroid hormones. There was no correlation between *Foxp3* and *Ccr5* mRNAs, which is unsurprising as several leukocytes other than Treg cells also express CCR5, including macrophages, DCs, and granulocytes. Significant correlations between *Foxp3* mRNA and *Ccr4* and *Itgae* mRNAs suggest these molecules might be involved in the migration or entrapment of Treg cells in the peri-implantation period, consistent with Treg cell regulation in other tissues [24, 60]. Other chemokines participate in Treg cell recruitment, and substantial redundancy in their actions is likely. After implantation, CXCL12 (SDF-1) expression in trophoblast is thought to attract Treg cells via their expression of CXCR4 receptors [61]. Further studies to investigate these molecules in the peri-implantation uterus will be informative.

Cumulatively, these results provide evidence for two mechanisms controlled by seminal fluid that act in synergy to achieve the increase in uterine $FOXP3^+$ Treg cells required for embryo implantation. First, seminal plasma elicits an increase in generation of Treg cells within the uterus-draining para-aortic LNs, resulting in greater availability of Treg cells for recruitment into the uterus. Second, seminal fluid-induced up-regulation of CCL19 in glandular epithelial cells would selectively promote migration of Treg cells from the circulation into the endometrium. A third mechanism might involve proliferation of recruited Treg cells in situ, and a recent report using the proliferation marker Ki67 suggests that local proliferation does indeed contribute to the uterine $FOXP3^+$ cell population [6].

In summary, this study provides new insights into the role of seminal fluid in facilitating pregnancy through regulating $FOXP3^+$ Treg cell accumulation in the implantation site. Given the critical role that Treg cells play in establishing pregnancy [4], a better understanding of the biological processes generating immune tolerance at embryo implantation will ultimately contribute to developing new diagnostics and treatments for implantation failure, miscarriage and other pathologies of pregnancy where an immune etiology is implicated.

REFERENCES

1. Trowsdale J, Betz AG. Mother's little helpers: mechanisms of maternal-fetal tolerance. Nat Immunol 2006; 7:241–246.
2. Aluvihare VR, Kallikourdis M, Betz AG. Regulatory T cells mediate maternal tolerance to the fetus. Nat Immunol 2004; 5:266–271.
3. Zhao JX, Zeng YY, Liu Y. Fetal alloantigen is responsible for the expansion of the $CD4^+CD25^+$ regulatory T cell pool during pregnancy. J Reprod Immunol 2007; 75:71–81.
4. Guerin LR, Prins JR, Robertson SA. Regulatory T-cells and immune tolerance in pregnancy: a new target for infertility treatment? Hum Reprod Update 2009; 15:517–535.
5. Shevach EM. $CD4^+CD25^+$ Suppressor T cells: more questions than answers. Nature Rev Immunol 2002; 2:389–400.
6. Shima T, Sasaki Y, Itoh M, Nakashima A, Ishii N, Sugamura K, Saito S. Regulatory T cells are necessary for implantation and maintenance of early

pregnancy but not late pregnancy in allogeneic mice. J Reprod Immunol 2010; 85:121–129.
7. Sakaguchi S, Sakaguchi N, Asano M, Itoh M, Toda M. Immunologic self-tolerance maintained by activated T cells expressing IL-2 receptor alpha-chains (CD25). Breakdown of a single mechanism of self-tolerance causes various autoimmune diseases. J Immunol 1995; 155:1151–1164.
8. Fontenot JD, Gavin MA, Rudensky AY. Foxp3 programs the development and function of $CD4^+CD25^+$ regulatory T cells. Nat Immunol 2003; 4:330–336.
9. Fontenot JD, Rasmussen JP, Williams LM, Dooley JL, Farr AG, Rudensky AY. Regulatory T cell lineage specification by the forkhead transcription factor foxp3. Immunity 2005; 22:329–341.
10. Akbar AN, Taams LS, Salmon M, Vukmanovic-Stejic M. The peripheral generation of $CD4^+$ $CD25^+$ regulatory T cells. Immunology 2003; 109:319–325.
11. Thornton AM, Shevach EM. $CD4^+CD25^+$ immunoregulatory T cells suppress polyclonal T cell activation in vitro by inhibiting interleukin 2 production. J Exp Med 1998; 188:287–296.
12. Walker LSK, Chodos A, Eggena M, Dooms H, Abbas AK. Antigen-dependent proliferation of $CD4^+$ $CD25^+$ regulatory T cells in vivo. J Exp Med 2003; 198:249–258.
13. Robertson SA, Guerin LR, Bromfield JJ, Branson KM, Ahlstrom AC, Care AS. Seminal fluid drives expansion of the $CD4^+CD25^+$ T regulatory cell pool and induces tolerance to paternal alloantigens in mice. Biol Reprod 2009; 80:1036–1045.
14. Johansson M, Bromfield JJ, Jasper MJ, Robertson SA. Semen activates the female immune response during early pregnancy in mice. Immunol 2004; 112:290–300.
15. Pandya IJ, Cohen J. The leukocytic reaction of the human uterine cervix to spermatozoa. Fertil Steril 1985; 43:417–421.
16. Sharkey DJ, Macpherson AM, Tremellen KP, Robertson SA. Seminal plasma differentially regulates inflammatory cytokine gene expression in human cervical and vaginal epithelial cells. Mol Hum Reprod 2007; 13:491–501.
17. Robertson SA. Seminal plasma and male factor signalling in the female reproductive tract. Cell and Tissue Res 2005; 322:43–52.
18. Beer AE, Billingham RE. Host responses to intra-uterine tissue, cellular and fetal allografts. J Reprod Fertil Suppl 1974; 21:59–88.
19. Moldenhauer LM, Diener KR, Thring DM, Brown MP, Hayball JD, Robertson SA. Cross-presentation of male seminal fluid antigens elicits T cell activation to initiate the female immune response to pregnancy. J Immunol 2009; 182:8080–8093.
20. Thuere C, Zenclussen ML, Schumacher A, Langwisch S, Schulte-Wrede U, Teles A, Paeschke S, Volk H-D, Zenclussen AC. Kinetics of regulatory T cells during murine pregnancy. Am J Reprod Immunol 2007; 58:514–523.
21. Robertson SA, Mau VJ, Tremellen KP, Seamark RF. Role of high molecular weight seminal vesicle proteins in eliciting the uterine inflammatory response to semen in mice. J Reprod Fertil 1996; 107:265–277.
22. Moldenhauer LM, Keenihan SN, Hayball JD, Robertson SA. GM-CSF is an essential regulator of T cell activation competence in uterine dendritic cells during early pregnancy in mice. J Immunol 2010; 185:7085–7096.
23. Jasper MJ, Tremellen KP, Robertson SA. Primary unexplained infertility is associated with reduced expression of the T-regulatory cell transcription factor Foxp3 in endometrial tissue. Mol Hum Reprod 2006; 12:301–308.
24. Suffia I, Reckling SK, Salay G, Belkaid Y. A role for CD103 in the retention of $CD4^+CD25^+$ Treg and control of Leishmania major infection. J Immunol 2005; 174:5444–5455.
25. Tafuri A, Alferink J, Moller P, Hammerling GJ, Arnold B. T cell awareness of paternal alloantigens during pregnancy. Science 1995; 270:630–633.
26. Erlebacher A, Vencato D, Price KA, Zhang D, Glimcher LH. Constraints in antigen presentation severely restrict T cell recognition of the allogeneic fetus. J Clin Invest 2007; 117:1399–1411.
27. Robertson SA. Immune regulation of conception and embryo implantation-all about quality control? J Reprod Immunol 2010; 85:51–57.
28. Hancock RJ, Faruki S. Assessment of immune responses to H-Y antigen in naturally inseminated and sperm-injected mice using cell-mediated cytotoxicity assays. J Reprod Immunol 1986; 9:187–194.
29. Zenclussen AC, Gerlof K, Zenclussen ML, Sollwedel A, Bertoja AZ, Ritter T, Kotsch K, Leber J, Volk HD. Abnormal T-cell reactivity against paternal antigens in spontaneous abortion: adoptive transfer of pregnancy-induced $CD4^+CD25^+$ T regulatory cells prevents fetal rejection in a murine abortion model. Am J Pathol 2005; 166:811–822.
30. Clark DA, Fernandez J, Banwatt D. Prevention of Spontaneous Abortion in the CBA x DBA/2 mouse model by intravaginal TGF-beta and local recruitment of $CD4^+CD8^+FOXP3^+$ cells. Am J Reprod Immunol 2008; 59:525–534.
31. Heikkinen J, Mottonen M, Alanen A, Lassila O. Phenotypic characterization of regulatory T cells in the human decidua. Clin Exp Immunol 2004; 136:373–378.
32. Somerset DA, Zheng Y, Kilby MD, Sansom DM, Drayson MT. Normal human pregnancy is associated with an elevation in the immune suppressive $CD25^+$ $CD4^+$ regulatory T-cell subset. Immunol 2004; 112:38–43.
33. Caruso A, Licenziati S, Corulli M, Canaris AD, Francesco MAD, Fiorentini S, Peroni L, Fallacara F, Dima F, Balsari A, Turano A. Flow cytometric analysis of activation markers on stimulated T cells and their correlation with cell proliferation. Cytometry 1997; 27:71–76.
34. Nishioka T, Shimizu J, Iida R, Yamazaki S, Sakaguchi S. $CD4^+CD25^+Foxp3^+$ T cells and $CD4^+CD25$-$Foxp3^+$ T cells in aged mice. J Immunol 2006; 176:6586–6593.
35. Hutter H, Dohr G. HLA expression on immature and mature human germ cells. J Reprod Immunol 1998; 38:101–122.
36. Robertson SA, Ingman WV, O'Leary S, Sharkey DJ, Tremellen KP. Transforming growth factor beta—a mediator of immune deviation in seminal plasma. J Reprod Immunol 2002; 57:109–128.
37. Siegmund K, Feuerer M, Siewert C, Ghani S, Haubold U, Dankof A, Krenn V, Schon MP, Scheffold A, Lowe JB, Hamann A, Syrbe U, et al. Migration matters: regulatory T-cell compartmentalization determines suppressive activity in vivo. Blood 2005; 106:3097–3104.
38. Annunziato F, Cosmi L, Liotta F, Lazzeri E, Manetti R, Vanini V, Romagnani P, Maggi E, Romagnani S. Phenotype, localization, and mechanism of suppression of CD4(+)CD25(+) human thymocytes. J Exp Med 2002; 196:379–387.
39. Mantovani A. The chemokine system: redundancy for robust outputs. Immunol Today 1999; 20:254–257.
40. Bono MR, Elgueta R, Sauma D, Pino K, Osorio F, Michea P, Fierro A, Rosemblatt M. The essential role of chemokines in the selective regulation of lymphocyte homing. Cytokine Growth Factor Rev 2007; 18:33–43.
41. Curiel TJ, Coukos G, Zou L, Alvarez X, Cheng P, Mottram P, Evdemon-Hogan M, Conejo-Garcia JR, Zhang L, Burow M, Zhu Y, Wei S, et al. Specific recruitment of regulatory T cells in ovarian carcinoma fosters immune privilege and predicts reduced survival. Nat Med 2004; 10:942–949.
42. Robertson SA, Allanson M, Mau VJ. Molecular regulation of uterine leukocyte recruitment during early pregnancy in the mouse uterus. Trophoblast Res 1998; 11:101–119.
43. Wood GW, Hausmann EH, Kanakaraj K. Expression and regulation of chemokine genes in the mouse uterus during pregnancy. Cytokine 1999; 11:1038–1045.
44. Kallikourdis M, Betz AG. Periodic accumulation of regulatory T cells in the uterus: preparation for the implantation of a semi-allogeneic fetus? PLoS ONE 2007; 2:e382.
45. Yurchenko E, Tritt M, Hay V, Shevach EM, Belkaid Y, Piccirillo CA. CCR5-dependent homing of naturally occurring $CD4^+$ regulatory T cells to sites of Leishmania major infection favors pathogen persistence. J Exp Med 2006; 203:2451–2460.
46. Forster R, Davalos-Misslitz AC, Rot A. CCR7 and its ligands: balancing immunity and tolerance. Nat Rev Immunol 2008; 8:362–371.
47. Fu S, Yopp AC, Mao X, Chen D, Zhang N, Mao M, Ding Y, Bromberg JS. $CD4^+$ $CD25^+$ $CD62^+$ T-regulatory cell subset has optimal suppressive and proliferative potential. Am J Transplant 2004; 4:65–78.
48. Link A, Vogt TK, Favre S, Britschgi MR, Acha-Orbea H, Hinz B, Cyster JG, Luther SA. Fibroblastic reticular cells in lymph nodes regulate the homeostasis of naive T cells. Nat Immunol 2007; 8:1255–1265.
49. Gunn MD, Tangemann K, Tam C, Cyster JG, Rosen SD, Williams LT. A chemokine expressed in lymphoid high endothelial venules promotes the adhesion and chemotaxis of naive T lymphocytes. Proc Natl Acad Sci U S A 1998; 95:258–263.
50. Shang L, Thirunarayanan N, Viejo-Borbolla A, Martin AP, Bogunovic M, Marchesi F, Unkeless JC, Ho Y, Furtado GC, Alcami A, Merad M, Mayer L, et al. Expression of the chemokine binding protein M3 promotes marked changes in the accumulation of specific leukocytes subsets within the intestine. Gastroenterology 2009; 137:1006–1018.
51. Bouma G, Coppens JM, Mourits S, Nikolic T, Sozzani S, Drexhage HA, Versnel MA. Evidence for an enhanced adhesion of DC to fibronectin and a role of CCL19 and CCL21 in the accumulation of DC around the pre-diabetic islets in NOD mice. Eur J Immunol 2005; 35:2386–2396.
52. Alt C, Laschinger M, Engelhardt B. Functional expression of the lymphoid chemokines CCL19 (ELC) and CCL 21 (SLC) at the blood-brain barrier suggests their involvement in G-protein-dependent lymphocyte recruit-

ment into the central nervous system during experimental autoimmune encephalomyelitis. Eur J Immunol 2002; 32:2133–2144.
53. Engelhardt B. Molecular mechanisms involved in T cell migration across the blood-brain barrier. J Neural Transm 2006; 113:477–485.
54. Daikoku N, Kitaya K, Nakayama T, Fushiki S, Honjo H. Expression of macrophage inflammatory protein-3beta in human endometrium throughout the menstrual cycle. Fertil Steril 2004; 81(suppl 1):876–881.
55. Luther SA, Bidgol A, Hargreaves DC, Schmidt A, Xu Y, Paniyadi J, Matloubian M, Cyster JG. Differing activities of homeostatic chemokines CCL19, CCL21, and CXCL12 in lymphocyte and dendritic cell recruitment and lymphoid neogenesis. J Immunol 2002; 169:424–433.
56. Yeaman GR, Guyre PM, Fanger MW, Collins JE, White HD, Rathbun W, Orndorff KA, Gonzalez J, Stern JE, Wira CR. Unique $CD8^+$ T cell-rich lymphoid aggregates in human uterine endometrium. J Leukoc Biol 1997; 61:427–435.
57. Yu CR, Mahdi RM, Liu X, Zhang A, Naka T, Kishimoto T, Egwuagu CE. SOCS1 regulates CCR7 expression and migration of $CD4^+$ T cells into peripheral tissues. J Immunol 2008; 181:1190–1198.
58. Debes GF, Arnold CN, Young AJ, Krautwald S, Lipp M, Hay JB, Butcher EC. Chemokine receptor CCR7 required for T lymphocyte exit from peripheral tissues. Nat Immunol 2005; 6:889–894.
59. Kallikourdis M, Andersen KG, Welch KA, Betz AG. Alloantigen-enhanced accumulation of $CCR5^+$ ''effector'' regulatory T cells in the gravid uterus. Proc Natl Acad Sci U S A 2007; 104:594–599.
60. Iellem A, Mariani M, Lang R, Recalde H, Panina-Bordignon P, Sinigaglia F, D'Ambrosio D. Unique chemotactic response profile and specific expression of chemokine receptors CCR4 and CCR8 by CD4(+)CD25(+) regulatory T cells. J Exp Med 2001; 194:847–853.
61. Lin Y, Xu L, Jin H, Zhong Y, Di J, Lin QD. CXCL12 enhances exogenous $CD4^+CD25^+$ T cell migration and prevents embryo loss in nonobese diabetic mice. Fertil Steril 2009; 91:2687–2696.
62. Mouse Genome Informatics, The Jackson Laboratory, Bar Harbor, ME. World Wide Web (URL: http://www.informatics.jax.org/). (January 2011).